

# Gravitational scattering in the ADD model at high and low energies

G. Gustafson<sup>1,a</sup>, M. Sjö Dahl<sup>2,b</sup>

<sup>1</sup> Department of Theoretical Physics, Lund University, Sölvegatan 14A, 22362 Lund, Sweden

<sup>2</sup> School of Physics and Astronomy, University of Manchester, Oxford Road, Manchester, M13 9PL, UK

Received: 21 August 2007 /

Published online: 7 November 2007 – © Springer-Verlag / Società Italiana di Fisica 2007

**Abstract.** Gravitational scattering in the ADD model is considered at both sub- and transplanckian energies using a common formalism. By keeping a physical cut-off in the KK tower associated with virtual KK exchange, such as the cut-off implied by a finite brane width, troublesome divergences are removed from the calculations in both energy ranges. The scattering behavior depends on three different energy scales: the fundamental Planck mass, the collision energy and the inverse brane width. The result for energies low compared to the effective cut-off (inverse brane width) is a contact-like interaction. At high energies the gravitational scattering associated with the extra dimensional version of Newton's law is recovered.

## 1 Introduction

The ADD model [1–3] is an attempt to solve the hierarchy problem by introducing extra dimensions in which only gravity is allowed to propagate. For distances smaller than the assumed compactification radius,  $R^1$ , the gravitational potential will then be altered and has the form

$$\frac{V(r)}{m_1 m_2} = -G_{N(4)} R^n S_n \frac{\Gamma(n)}{r^{n+1}}, \quad (1)$$

where  $n$  is the number of extra dimensions,  $G_{N(4)}$  denotes the ordinary 3 + 1-dimensional Newton's constant,  $S_n = 2\pi^{n/2}/\Gamma(n/2)$  is the surface of a unit sphere in  $n$  dimensions and  $\Gamma(n)$  is the Euler Gamma function. This implies that the strength of gravity increases much faster with smaller distance as compared with the normal  $1/r$  behavior, and the fundamental Planck scale (related to the mass scale where the corresponding de Broglie wave length equals the black hole radius) is reduced and given by

$$M_D = \frac{1}{(8\pi R^n G_{N(4)})^{\frac{1}{n+2}}}. \quad (2)$$

The presence of strong gravity at distances smaller than the compactification radius opens up the possibility of observing gravitational scattering and black hole production at collider experiments and in cosmic rays. To eliminate

the hierarchy problem, and not only reduce it, the new Planck scale should be of the order of TeV, and LHC will be a quantum gravity probing machine.

In order to quantify the amount of gravitational interaction, the theory was formulated as a field theory in [5, 6]. As the extra dimensions are compactified, the allowed wave numbers (and hence momenta) in these dimensions are quantized Kaluza–Klein (KK) modes. The KK modes can of course enter both as external and internal particles in the Feynman diagrams derived from the theory. When the KK modes are internal (as for elastic gravitational scattering) they have to be summed over. The problem is that the sum over KK modes diverges for 2 or more extra dimensions,

$$\sum_{\vec{l}} \frac{1}{-m_{\vec{l}}^2 + k^2} = S_n R^n \int \frac{m^{n-1}}{-m^2 + k^2} dm. \quad (3)$$

Here  $\vec{l}$  enumerates the allowed KK modes with momenta  $m_{\vec{l}}$  in the extra dimensions,  $m = |m_{\vec{l}}|$ , and  $k$  is the exchanged 4-momentum in our normal space. (We will for simplicity call this object a propagator, despite the fact that the Lorentz structure is not included.)

In the original papers [5, 6] this divergence problem was dealt with by introducing a sharp cut-off,  $M_s$ , argued to be of the same order of magnitude as the Planck mass, as new physics anyhow is expected to occur at the Planck scale. Various mathematical forms of cut-offs have also been discussed in [7]. For  $n \geq 3$  and momentum transfers small compared to  $M_s$ , the sum was then estimated to give

$$\sim \frac{1}{n-2} R^n M_s^{n-2} \approx \frac{1}{G_{N(4)}(n-2)} \frac{M_s^{n-2}}{M_D^{n+2}}. \quad (4)$$

<sup>a</sup> e-mail: gosta.gustafson@thep.lu.se

<sup>b</sup> e-mail: malin.sjodahl@manchester.ac.uk

<sup>1</sup> Here we use the notation of [4], so that  $R$  is the radius and not the circumference.

In the Born approximation this would lead to a cross section of the form [8]

$$\frac{d\sigma}{dz} \sim \frac{s^3}{(n-2)^2} \left( \frac{M_s^{n-2}}{M_D^{n+2}} \right)^2 F(\text{spin}, z), \quad (5)$$

where  $z$  is cosine of the scattering angle in the center of mass system,  $\sqrt{s}$  the total CMS energy, and  $F$  a function taking spin dependence into account.

Ordinary gravitational scattering in  $3+n$  dimensions would correspond to a potential  $\propto 1/r^{(n+1)}$ , but the scattering given by (5) has a completely different angular behavior. In particular the expected forward peak is totally absent. Fourier transforming the amplitude in (4) to position gives a  $\delta$ -function potential,  $\propto \delta(\bar{r})$ , and the corresponding Born approximation cross section in (5) is therefore isotropic. Thus it is obvious that the approximation in (4) does not contain the full story of gravitational scattering in the ADD model.

This problem was considered in [4] by Giudice, Rattazzi, and Wells. These authors point out two important facts.

- i) For an interaction with a large Born amplitude but a short range, the cross section is not determined by the Born term alone. Higher order loop corrections are important to keep the cross section within the unitarity limits.
- ii) The constant term in (4), which represents a dominant part of the amplitude in (3), corresponds to a contribution to the cross section from zero impact parameter, and should therefore give a negligible contribution to the cross section when the incoming wave packages do not overlap. Consequently the important part of the amplitude in (3) must in this case be the smaller  $k$ -dependent terms, which have been neglected in (4).

In case the interaction is dominated by small angle scattering the cross section can be calculated in the eikonal approximation, in which the all-loop summation exponentiates [9–11]. The cross section is then given by

$$\sigma_{\text{el}} = \int d^2\bar{b}_\perp \left| \left( 1 - e^{i\chi(\bar{b}_\perp)} \right) \right|^2, \quad (6)$$

$$\sigma_{\text{tot}} = \int d^2\bar{b}_\perp 2 \text{Re} \left( 1 - e^{i\chi(\bar{b}_\perp)} \right), \quad (7)$$

$$\chi(\bar{b}_\perp) = \frac{1}{2s} \int \frac{d^2\bar{q}_\perp}{(2\pi)^2} e^{i\bar{q}_\perp \cdot \bar{b}_\perp} A_{\text{Born}}(\bar{q}_\perp^2). \quad (8)$$

Thus, if the absolute value of the eikonal,  $\chi$ , is small compared to 1, we in general expect small corrections from the higher order loop contributions, while for large  $\chi$ -values the cross section saturates, and the effective integrand in (6) is close to 1. We also note that when  $\chi$  is real, the scattering is purely elastic. In this paper we will focus on elastic collisions mediated via (multiple) exchange in the  $t$ -channel.

It is also pointed out in [4] that in the eikonal limit the Born amplitude does not depend on the spin of the colliding particles and is therefore universal. Expressed in the

fundamental Planck mass  $M_D$  in (2) it is given by [4]

$$A_{\text{Born}}(k^2) = \frac{s^2}{M_D^{n+2}} \int \frac{d^n \bar{m}}{k^2 - \bar{m}^2}. \quad (9)$$

In [4] a divergent part is subtracted from the integral in (3) or (9) using dimensional regularization. This subtracted part corresponds to a narrow potential localized at  $\bar{r} = 0$ . Although the remainder is singular for  $n$  equal to an even integer, its Fourier transform (the eikonal  $\chi$  in (8)) is finite everywhere. Assuming the eikonal approximation to be applicable in the transplanckian region  $s \gg M_D^2$ , the authors of [4] thus obtain a reasonable result, where the gravitational scattering cross section grows with energy  $\propto (s/M_D^{n+2})^{2/n}$ . However, we ought to be worried by the fact that the part of the amplitude, remaining after the subtraction, grows for larger momentum transfers, and is largest for backward scattering. This implies that the conditions for the eikonal approximation are not satisfied. These uncertainties also make it difficult to estimate the limit beyond which the result should be applicable, and how the gravitational scattering behaves for lower energies.

In this paper we want to study in more detail the result of physical effects, which can tame the divergences. These effects give effective cut-offs for high-mass KK modes at some scale (here referred to as  $M_s$ ), which does not have to be the same as the Planck scale  $M_D$ . Our result does indeed confirm the relevance of the eikonal approximation and the result in [4] at high energies. For lower energies the behavior is different, wide-angle scattering is dominant and the amplitude does not exponentiate. Instead a (brane related) regularization implies that a summation of the  $s$ -channel ladder diagrams give a geometric series. This means that there will be a change in the energy dependence, and for lower energies the cross section varies more rapidly, proportional to  $\propto s^2 M_s^{2n-2} / M_D^{2n+4}$ .

We want to emphasize that in this paper we do not discuss phenomena like black hole formation or other non-linear gravitational effects, which are expected to modify the final states for very high energies and central collisions. For a discussion of such effects we refer to [3, 4, 12–17]. We also neglect possible interference with strong and electroweak effects and we study reactions for non-identical particles such that KK modes appears only in the  $t$ -channel. Some remarks on  $s$ - and  $u$ -channels are however made in Sects. 6.3–6.5.

The approach in [4] will be discussed in more detail in Sect. 2. In Sect. 3, we will introduce a finite width of the brane, on which the standard model particles are assumed to live, and see how this leads to a finite amplitude. A similar effect is obtained by assuming that the position of the brane is not fixed in the extra dimensions [18, 19]. Fluctuations in the brane then result in a kind of surface tension or “brane tension”.

The Born term is discussed in Sect. 4 and higher order loop corrections in Sect. 5. Here we also study in which kinematical regions the Born term dominates, where the eikonal approximation is valid, and the behavior of the cross section in regions where the scattering is approximately isotropic. The results for scattering cross sections

in those different kinematical regions are then presented in Sect. 6. Finally we will summarize and conclude in Sect. 7.

## 2 Problems and divergences

The integral in (3) or (9) is divergent for  $n \geq 2$  and  $n \leq 0$  but converges for  $n$ -values in the intermediate range  $0 < n < 2$ . To give a physical meaning to the integral for  $n \geq 2$ , a finite result can be obtained by analytic continuation from smaller  $n$ -values, corresponding to a dimensional regularization. The resulting amplitude, presented in [4], is given by the expression<sup>2</sup>

$$A_{\text{Born}}(k^2) = -\pi^{\frac{n}{2}} \Gamma\left(1 - \frac{n}{2}\right) \left(\frac{-k^2}{M_{\text{D}}^2}\right)^{\frac{n}{2}-1} \left(\frac{s}{M_{\text{D}}^2}\right)^2. \quad (10)$$

We see that this expression is finite for odd integers  $n$ , but singular for even  $n$ , where the  $\Gamma$ -function has poles.

The result in (10) is equivalent to a subtraction of terms, which are proportional to  $\delta$ -functions or derivatives of  $\delta$ -functions at  $\bar{r} = \bar{0}$ , and therefore may be expected to give small contributions to the cross section. Ignoring these short distance terms we can, however, not expect a smooth transition between high and low energies, since at low energies contributions from overlapping wave functions will be important, (cf. (29) below). Inserting (10) into the 2-dimensional Fourier transform in (8), we see that this integral is also divergent. It can be given a finite result by introduction of a convergence factor:

$$\chi = -\left(\frac{b_{\text{c}}}{b}\right)^n, \quad b_{\text{c}} = \left[\frac{s(4\pi)^{\frac{n}{2}-1} \Gamma(n/2)}{2M_{\text{D}}^{n+2}}\right]^{1/n}. \quad (11)$$

We note that although the amplitude  $A_{\text{Born}}$  in (10) is singular for even  $n$ ,  $\chi$  is finite. Thus  $\chi(b)$  (like the potential  $V(r)$ , to be discussed below) can be analytically continued to finite values for all  $n$ -values. (A finite amplitude, which corresponds to a potential proportional to  $1/r^{n+1}$  for  $n$  even, is  $\propto (-k^2)^{n/2-1} \ln(-k^2)$ .)

The result in (11) is a single power  $\propto 1/b^n$ , and the scale factor (or characteristic impact parameter)  $b_{\text{c}}$  is defined so that  $|\chi| = 1$  when  $b = b_{\text{c}}$ . If this expression is inserted into (6), we see that the term quadratic in  $\chi$ , which is the Born term, dominates the integrand for  $b > b_{\text{c}}$ , where  $\chi < 1$ , but higher order corrections are important in constraining the scattering probability for  $b < b_{\text{c}}$ .

In [4] it is argued that (6) and (11) should give a realistic approximation to gravitational scattering in the transplanckian region  $s \gg M_{\text{D}}^2$  (apart from special effects like black hole formation, which are treated separately). The net result is then that the total scattering cross section grows with energy proportional to  $b_{\text{c}}^2$ , or equivalently  $\propto (s/M_{\text{D}}^{n+2})^{2/n}$  (cf. (44) below).

The exponentiation in the eikonal approximation in (6) follows when the scattering is dominated by small angles [9–11]. The one-loop contribution is then dominated

by its imaginary part, and the all-loop summation gives an exponential.

The one-loop diagram in Fig. 1a is given by the following expression:

$$A_{1\text{-loop}}(k^2) = \frac{-i}{2} \int \frac{d^4 q}{(2\pi)^4} A_{\text{Born}}(q^2) A_{\text{Born}}((k-q)^2) \times \frac{1}{(p_1 - q)^2} \frac{1}{(p_2 + q)^2}. \quad (12)$$

Here  $p_1$  and  $p_2$  denote the momenta of the incoming particles, the total momentum exchange is  $k$  and the loop momentum  $q$ . The imaginary part of the integral in (12) is coming from on-shell intermediate states (denoted  $i$  in Fig. 1), and can be calculated using the Cutkosky cutting rules. This implies that the two propagators in (12) are replaced by  $\delta$ -functions, which (with the approximation  $q^2 \approx -\bar{q}_{\perp}^2$ ) gives the result

$$\text{Im } A_{1\text{-loop}}(k^2) = \frac{i}{4s} \int_{q_{\perp} < \sqrt{s}/2} \frac{d^2 \bar{q}_{\perp}}{(2\pi)^2} \times A_{\text{Born}}(-\bar{q}_{\perp}^2) A_{\text{Born}}(-(\bar{k}_{\perp} - \bar{q}_{\perp})^2). \quad (13)$$

The restriction to physical intermediate states implies that the integral is limited to the region  $q_{\perp} < \sqrt{s}/2$ , but if  $A_{\text{Born}}$  falls off for large  $q_{\perp}$  the finite integral in (13) can be approximated by an integral over all  $q_{\perp}$ . This implies that the Fourier transform to impact parameter space of the one-loop contribution is proportional to  $\chi^2(\bar{b}_{\perp})$ . The sum over multi-loop ladder diagrams with different number of KK exchanges then exponentiates to  $(i\chi - \chi^2/2 + \dots) = e^{i\chi} - 1$ , and the all order eikonal amplitude is given by

$$A_{\text{eik}}(k^2) = -2is \int d^2 \bar{b}_{\perp} e^{i\bar{k}_{\perp} \cdot \bar{b}_{\perp}} (e^{i\chi} - 1). \quad (14)$$

With the Born amplitude in (10) we have, however, some problems. The amplitude in (10) does not fall off for large  $k_{\perp}$ . Therefore the real part of the integral in (12) is not small and negligible compared to the imaginary part. It is strongly divergent for  $n \geq 2$ , as  $A_{\text{Born}}$  increases proportional to  $q^{n-2}$  or  $q^{n-2} \ln(-q^2)$  for large  $q$ . For the imaginary part the integral in (13) cannot be extended to infinity, and the Fourier transform of the convolution in (13) is not given by  $\chi^2$ .

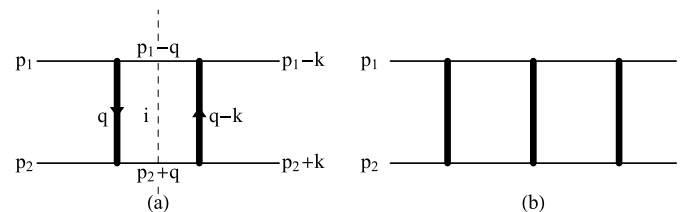


**Fig. 1.** **a** The one-loop contribution corresponding to exchange of two KK modes. The KK modes are drawn as *thick lines* and standard model particles as *thin lines*. **b** The two-loop contribution

<sup>2</sup> We have here inserted a minus sign not present in [4].

We conclude that, although the result in (11) and (6) is an intuitively reasonable result for scattering in a rapidly falling potential, it should be worrying that it is derived from an amplitude that grows for large momentum transfers and large scattering angles, while the eikonal approximation is proven to be valid only when scattering at small angles is dominating.

At the root of this problem lies the fact that the subtraction, which gives the amplitude in (10) and is a result of the analytic continuation in the number of extra dimensions, does *not* automatically remove all parts corresponding to  $\delta$ -functions at  $\bar{r} = 0$ . The definition of the potential as the Fourier transform of (10) is problematic. To illustrate this we study the most simple example represented by the case  $n = 3$ . In the rest frame we have  $k_0 = 0$  and  $k^2 = -\bar{k}^2$ . The integral in (9) is then proportional to

$$\begin{aligned} \int \frac{m^2 dm}{\bar{k}^2 + m^2} &= \int \frac{(m^2 + \bar{k}^2 - \bar{k}^2) dm}{\bar{k}^2 + m^2} \\ &= \int dm - \bar{k}^2 \int \frac{dm}{\bar{k}^2 + m^2} \\ &= \int dm - |\bar{k}| \int \frac{dx}{1+x^2} \\ &= \int dm - |\bar{k}| \frac{\pi}{2}. \end{aligned} \quad (15)$$

The first term, the integral, represents an infinite subtraction. Its 3-dimensional Fourier transform gives a  $\delta$ -function at  $\bar{r} = 0$  with an infinite weight. The second term corresponds to the result in (10). We may try to define its Fourier transform  $\hat{V}(\bar{r})$  as a distribution in the standard way, multiplying with a test function and interchanging the order of integration. For test functions of the form  $\exp(-a r^2)$  we then get (with  $k \equiv |\bar{k}|$  and the constant  $C$  appearing in (26))

$$\begin{aligned} \int d^3 r e^{-ar^2} \hat{V}(\bar{r}) &\equiv C \left(-\frac{\pi}{2}\right) \int d^3 k k \int d^3 r e^{-ar^2} e^{i\bar{r}\bar{k}} \\ &= -C \frac{\pi}{2} \int d^3 k k e^{-k^2/4a} \left(\frac{\pi}{a}\right)^{\frac{3}{2}} \\ &= -C 16\pi^{\frac{7}{2}} \sqrt{a}. \end{aligned} \quad (16)$$

We note that this result is finite and goes towards 0 when the test function approaches a constant, i.e. when  $a \rightarrow 0$ . For  $r \neq 0$  we find  $\hat{V}(r) = C 4\pi^2/r^4$  by Fourier transforming from  $\bar{k}$  to  $\bar{r}$  using a convergence factor. Integrating this contribution with the test function above, we get the divergent result

$$C 16\pi^3 \int_0^\infty e^{-ar^2} \frac{dr}{r^2}. \quad (17)$$

Thus this definition,  $\hat{V}(r) = C 4\pi^2/r^4$  for  $r > 0$ , is incomplete since the result in (16) is finite while the integral in (17) is infinite. It looks as if a  $\delta$ -function,  $\delta(\bar{r})$ , with infinite weight is missing.

We conclude that the separation in (15) does not in itself remove all terms related to  $\delta$ -functions at  $\bar{r} = \bar{0}$ . Instead we argue in the next section that dynamical effects will remove the divergences in (9) and give finite results. These

mechanisms have real dynamical motivations, and we will see that such finite cut-offs do remove all divergences related to the extra dimensions. Divergences related to loop momenta in our ordinary dimensions are however not affected. For high energies the Born amplitude indeed falls off for large momentum transfers, and the eikonal approximation is applicable. For lower energies this is not the case, and we will in Sects. 4–6 discuss the resulting amplitudes and cross sections for different relations between the energy, the Planck mass, and the cut-off scale.

### 3 Possible solutions

In the ADD model the standard model particles are assumed to live on a thin brane. The mechanism behind this assumption could possibly be taken from string theory [3], but is not a part of the ADD model itself. The problems discussed in the previous section are related to contributions from KK modes with very high masses. In a relativistic quantized theory there are also formal problems with an infinitely thin and infinitely rigid brane. If the brane is not infinitely thin but has a finite width, this will effectively suppress the coupling to high-mass KK modes, with wavelengths shorter than the brane width. If the brane really is infinitely thin, then it must be impossible to determine its position with infinite accuracy. In [18, 19] it is demonstrated that the fluctuations in the position of the brane suppress high-mass KK modes, in a way similar to the effect of a finite brane width. The emission or absorption of a KK mode gives a recoil to the brane, and the fluctuations in the location of the brane can then be regarded as a result of an effective “surface tension” in the brane.

Let us for definiteness assume that the interaction can be described by an effective field theory, and that the standard model fields penetrate a finite distance into the extra dimensions, thus giving an effective finite width to the brane [20]. (The possibility of fluctuating branes, studied in [18, 19], give similar results, albeit with a different physical interpretation.) To be specific we assume a Gaussian extension, but this assumption is not essential for our conclusions. Thus we assume the standard model fields to have a wave function with the extension

$$\psi(\bar{y}) = \left(\frac{M_s}{\sqrt{2\pi}}\right)^{\frac{n}{2}} e^{-\bar{y}^2 M_s^2/4} \quad (18)$$

into the extra dimensions, with  $\bar{y}$  denoting the coordinate in the extra dimensions. The overlap between two standard model fields and a KK mode of mass  $m$  (what we have in a vertex) is then proportional to

$$\int d\bar{y} e^{i\bar{m}\cdot\bar{y}} \left(\frac{M_s}{\sqrt{2\pi}}\right)^{2\frac{n}{2}} e^{-\bar{y}^2 M_s^2/2} = e^{-m^2/(2M_s^2)}, \quad (19)$$

or, in other words, the squared absolute value of the wave function in  $\bar{y}$ -space Fourier transformed to  $m$ -space. The exchange of a KK mode will have this suppression factor occurring twice, once at every vertex. In total the exchange

of a KK mode with mass  $m$  will therefore contribute to the sum in (9) with a suppression factor

$$e^{-m^2/M_s^2}. \quad (20)$$

Implementing the physical requirement that the standard model particles live on a narrow brane does therefore in itself imply a finite “effective” propagator,

$$R^n S_n \int \frac{dmm^{n-1}}{k^2 - m^2} e^{-m^2/M_s^2} \quad (21)$$

for the exchange of 4-momentum  $k$ . (The factor  $R^n$  comes from the density of KK modes and  $S_n = 2\pi^{n/2}/\Gamma(n/2)$  is the unit surface of a sphere in  $n$  dimensions.) We note in particular that this expression (in contrast to the expression in (10)) falls off like  $1/k^2$  for large momentum transfers, such that  $-k^2 \gg M_s^2$ . This implies that for high energies,  $s \gg M_s^2$ ,  $t$ -channel interaction is dominated by small values of  $-k^2/s$ , i.e. by small angles.

In the following sections we will show that the Fourier transform of the propagator in (21) gives a potential that falls off  $\propto 1/r^{n+1}$  for distances larger than the brane width, given by  $1/M_s$ , and smaller than the compactification radius. Outside this range, both for  $r < 1/M_s$  and for  $r > 2\pi R$  (where the massless graviton dominates), it varies  $\propto 1/r$ . We will also study the resulting scattering cross sections under different kinematic conditions.

## 4 The Born term

### 4.1 Amplitude

As described in Sect. 3, several physical mechanisms result in effective cut-offs for high masses in the KK propagator. After multiplying (21) by the coupling  $4\pi G_{N(4)}$ , contracting Lorentz indices (not explicitly included here), and using the relation  $G_{N(4)}^{-1} = 8\pi R^n M_D^{2+n}$  we get the following result for the Born amplitude for ultra-relativistic small angle scattering:

$$A_{\text{Born}}(t) = \frac{s^2}{M_D^{n+2}} S_n \int_0^\infty \frac{dmm^{n-1}}{k^2 - m^2} e^{-m^2/M_s^2}. \quad (22)$$

For large angles there are less important corrections from spin polarization, which we neglect here and in the following. This integral is convergent and finite for all negative values of  $k^2 = t$  (including 0 when  $n \geq 3$ ). It is easy to find the result in the limits of large and small (negative)  $t$ -values.

– *Large momentum transfers,  $-t \gg M_s^2$*

When  $-t$  is large compared to  $M_s^2$ , the term  $m^2$  in the denominator in (22) can be neglected, which gives the result:

$$\begin{aligned} A_{\text{Born}}(t) &\approx \frac{s^2}{M_D^{n+2}} S_n \int_0^\infty \frac{dmm^{n-1}}{t} e^{-m^2/M_s^2} \\ &= \pi^{n/2} \left( \frac{M_s}{M_D} \right)^n \frac{s^2}{M_D^2 \cdot t}. \end{aligned} \quad (23)$$

Thus for large momentum transfers (larger than the cut-off) the Born amplitude falls off proportional to  $1/t$ .

– *Small momentum transfers,  $-t \ll M_s^2$*

For smaller  $t$ , and  $n > 2$ , the integral is dominated by  $m$ -values of the order of  $M_s$ , and therefore  $t$  can now be neglected in the denominator. We then get the approximately constant result:

$$\begin{aligned} A_{\text{Born}}(t) &\approx \frac{-s^2}{M_D^{n+2}} S_n \int_0^\infty dmm^{n-3} e^{-m^2/M_s^2} \\ &= -\frac{2\pi^{n/2}}{(n-2)} \left( \frac{M_s}{M_D} \right)^n \frac{s^2}{M_D^2 M_s^2}. \end{aligned} \quad (24)$$

Thus for momentum transfers that are small compared to the cut-off, the Born amplitude is approximately constant for  $n > 2$ . For  $n = 2$  the result for small  $t$  has instead a slowly varying logarithmic dependence, proportional to  $\ln(-M_s^2/t)$ .

### 4.2 Potential

To get the classical non-relativistic potential we start directly from the effective propagator in (21) multiplied with the coupling constant  $4\pi G_{N(4)}$ . Going to the rest frame, where  $k_0 = 0$  and  $t = -\vec{k}^2$  we find the corresponding potential as the 3-dimensional Fourier transform:

$$\begin{aligned} \frac{V(r)}{m_1 m_2} &= \frac{1}{2s^2} \int \frac{d^3 \vec{k}}{(2\pi)^3} e^{i\vec{k}\vec{r}} A_{\text{Born}}(-\vec{k}^2) \\ &= \frac{-1}{2M_D^{n+2}} \frac{S_n}{(2\pi)^3} \int_0^\infty dmm^{n-1} e^{-m^2/M_s^2} \int \frac{d^3 k e^{i\vec{k}\vec{r}}}{m^2 + \vec{k}^2} \\ &= \frac{-1}{2M_D^{n+2}} \frac{S_n}{(2\pi)^3} 2\pi^2 \int_0^\infty dmm^{n-1} e^{-m^2/M_s^2} \cdot \frac{e^{-mr}}{r}. \end{aligned} \quad (25)$$

This represents a weighted sum of Yukawa potentials. The integral can be expressed in terms of error functions, but we are here primarily interested in the behavior for large and small values of  $r$ .

– *Large distances,  $r > 1/M_s$*

For distances larger than the brane thickness the integral is effectively cut off by the factor  $e^{-mr}$ , and the result becomes insensitive to the Gaussian cut-off  $e^{-m^2/M_s^2}$ . It is then approximated by

$$\begin{aligned} \frac{V(r)}{m_1 m_2} &\approx \frac{-1}{2M_D^{n+2}} \frac{S_n}{4\pi} \int_0^\infty dmm^{n-1} \cdot \frac{e^{-mr}}{r} \\ &= \frac{-S_n \Gamma(n)}{8\pi M_D^{n+2}} \cdot \frac{1}{r^{n+1}}. \end{aligned} \quad (26)$$

We see that for distances large compared to the brane thickness (but small compared to the compactification radius) we recover the result from (1), a potential falling off proportional to  $1/r^{n+1}$ , corresponding to the expected  $(3+n)$ -dimensional version of Newton’s law. When  $r$  is increased, smaller  $m$ -values  $\sim 1/r$  are important in the integral in (25) or (26). The phase space

factor  $m^{n-1}$  then gives this power-like fall-off for distances large compared to  $M_s$ .

– *Short distances*,  $r < 1/M_s$

For smaller  $r$ -values we find instead that the factor  $e^{-mr}$  is irrelevant, and the result is

$$\begin{aligned} \frac{V(r)}{m_1 m_2} &= \frac{-1}{2M_D^{n+2}} \frac{S_n}{4\pi} \frac{1}{r} \int_0^\infty dmm^{n-1} e^{-m^2/M_s^2} \\ &= \frac{-\pi^{n/2}}{8\pi} \frac{M_s^n}{M_D^{n+2}} \cdot \frac{1}{r}. \end{aligned} \quad (27)$$

Due to the cut-off, the integral in (25) is dominated by  $m$ -values close to  $M_s$  for all  $r$ -values smaller than  $1/M_s$ . Thus, when the distance is smaller than the brane width, the result is a potential proportional to  $1/r$ , corresponding to a standard 3-dimensional Coulomb potential, although with a coupling constant  $\sim M_s^n/M_D^{n+2} \sim (M_s R)^n G_{N(4)}$  instead of  $G_{N(4)}$ . Thus the coupling is enhanced by a factor  $\sim (M_s R)^n = \left(\frac{\text{compactification radius}}{\text{brane width}}\right)^n$ .

### 4.3 Eikonal

In a similar way we can calculate the eikonal  $\chi(b)$  by a 2-dimensional Fourier transform in the transverse coordinates:

$$\begin{aligned} \chi(b) &= \frac{1}{2s} \int \frac{d^2 \bar{k}_\perp}{(2\pi)^2} e^{i\bar{k}_\perp \bar{b}_\perp} A_{\text{Born}}(-\bar{k}_\perp^2) \\ &= \frac{-s}{2M_D^{n+2}} \frac{S_n}{(2\pi)^2} \int_0^\infty dmm^{n-1} e^{-m^2/M_s^2} \\ &\quad \times \int d^2 \bar{k}_\perp e^{i\bar{k}_\perp \bar{b}_\perp} \frac{1}{m^2 + \bar{k}_\perp^2} \\ &= \frac{-s}{2M_D^{n+2}} \frac{S_n}{(2\pi)^2} 2\pi \int_0^\infty dmm^{n-1} e^{-m^2/M_s^2} \\ &\quad \times \int_0^\infty \frac{k_\perp dk_\perp}{m^2 + k_\perp^2} J_0(k_\perp b) \\ &= \frac{-s}{2M_D^{n+2}} \frac{S_n}{2\pi} \int_0^\infty dmm^{n-1} e^{-m^2/M_s^2} K_0(mb). \end{aligned} \quad (28)$$

This integral can be expressed in terms of confluent hypergeometric functions of the second kind:

$$\chi(b) = -\frac{sM_s^n}{M_D^{n+2}} \Gamma\left(\frac{n}{2}\right) \frac{\pi^{n/2-1}}{8} U\left(\frac{n}{2}, 1, \frac{M_s^2 b^2}{4}\right). \quad (29)$$

Note that this represents a smooth transition between high and low energies not possible to obtain by ignoring short distance terms. This expression can easily be used in numerical calculations. For an intuitive picture, the result for large and small  $b$ -values can be estimated in the same way as the approximations in (26) and (27).

– *Large impact parameters*,  $b \gg 1/M_s$

For large arguments the asymptotic behavior of the Bessel function  $K_0(mb)$  is proportional to  $\exp(-mb)/$

$\sqrt{mb}$ . This implies that for large  $b$  the Gaussian cut-off is unessential, and we find the eikonal

$$\begin{aligned} \chi(b) &\approx \frac{-s}{2M_D^{n+2}} \frac{S_n}{2\pi} \int dmm^{n-1} K_0(mb) \\ &= \frac{-s}{M_D^{n+2}} \frac{S_n}{\pi} 2^{n-4} \Gamma^2(n/2) \cdot \frac{1}{b^n} \\ &= \frac{-s}{2M_D^{n+2}} (4\pi)^{\frac{n}{2}-1} \Gamma\left(\frac{n}{2}\right) \cdot \frac{1}{b^n}. \end{aligned} \quad (30)$$

– *Small impact parameters*,  $b \ll 1/M_s$

For small arguments we have  $K_0(mb) \approx \ln(1/(mb))$ , which implies

$$\begin{aligned} \chi(b) &\approx \frac{-s}{2M_D^{n+2}} \frac{S_n}{2\pi} \int dmm^{n-1} e^{-m^2/M_s^2} \ln\left(\frac{1}{mb}\right) \\ &= \frac{\pi^{\frac{n}{2}-1}}{4} \frac{s}{M_D^2} \left(\frac{M_s}{M_D}\right)^n \left(\ln(M_s b) + \frac{1}{2} \psi\left(\frac{n}{2}\right)\right), \end{aligned} \quad (31)$$

where  $\psi(\frac{n}{2})$  is the psi or digamma function.

Thus we see that the eikonal falls off  $\propto 1/b^n$  for large  $b$ , and grows logarithmically when  $b \rightarrow 0$ . Using the quantity  $b_c$  from (11) and keeping only the dominant term  $\ln(M_s b)$  in (31), we can write the results in the form

$$\chi(b) \approx -\left(\frac{b_c}{b}\right)^n; \quad b > b_d \quad (32)$$

$$\chi(b) \approx \frac{-(b_c M_s)^n}{2^{n-1} \Gamma(n/2)} \ln\left(\frac{1}{M_s b}\right), \quad b < b_d \quad (33)$$

$$b_d \equiv \frac{1}{M_s}, \quad (34)$$

$$b_c \equiv \left[\frac{s(4\pi)^{\frac{n}{2}-1} \Gamma(n/2)}{2M_D^{n+2}}\right]^{1/n}. \quad (35)$$

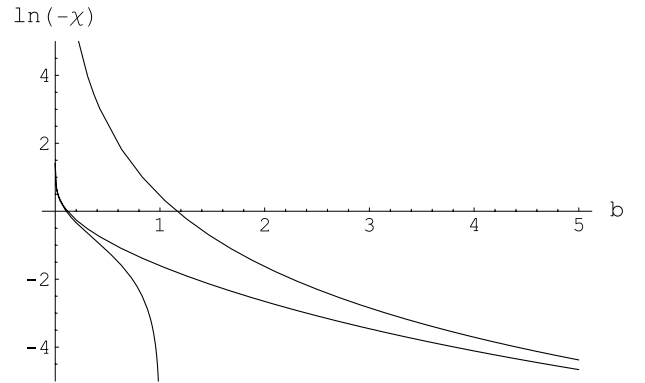


**Fig. 2.** The logarithm of  $|\chi|$  as a function of impact parameter for  $n=3$ . The curves show the example where  $\sqrt{s}$ ,  $M_D$ , and  $M_s$  have the same magnitude, and the units are chosen such that  $\sqrt{s} = M_D = M_s = 1$ . This also implies that  $b_d = 1$ . The *uppermost line* is the large  $b$  limit of  $\chi$  taken from (32) and the *lowermost line* is the small  $b$  limit of  $\chi$  taken from (33). The *interpolating line* is the exact expression (29). Note that a change in  $s$  and/or  $M_D$ , keeping  $M_s$  constant, just corresponds to shifting all curves up or down



The separation line  $b_d = 1/M_s$  is an estimate of the  $b$ -value where  $\chi(b)$  changes behavior. As an example Fig. 2 shows these approximations for  $\chi$  together with the exact result for  $n = 3$  and  $\sqrt{s} = M_D = 1$  in units such that  $M_s = 1$ . As  $\chi$  is proportional to  $s/M_D^{n+2}$ , a change in  $s$  and/or  $M_D$  just corresponds to a shift of all curves the same distance up or down.

## 5 Higher order loop corrections

We note that three different energy scales enter the expressions for the Born amplitude in (22) and (29):  $\sqrt{s}$ ,  $M_D$ , and  $M_s$ . Here  $\sqrt{s}$  is the total energy in the scattering,  $M_D$  is the fundamental Planck scale determined by the compactification radius  $R$ , and  $M_s$  is related to the width of the brane (or the brane tension). The result depends on the relative magnitude of these quantities, and in the following we will successively discuss five different kinematical regions, which are illustrated in Fig. 3.

### 5.1 Eikonal regions, $s \gg M_s^2$

We study the scattering process in the overall CM system, where the momentum exchange has no 0-component,  $k = (0; \vec{k})$  and  $t = -\vec{k}^2$ . From (23) we see that  $A_{\text{Born}}$  falls off  $\propto 1/\vec{k}^2$  for  $\vec{k}^2 > M_s^2$ . Thus for high energies, such that  $s \gg M_s^2$ , corresponding to region 1 and 2 in Fig. 3, the Born term is dominated by small values of  $\vec{k}^2/s$ , i.e. small angles. This implies that the eikonal approximation is applicable. We note in particular that it is  $M_s$  rather than  $M_D$ , that sets the scale

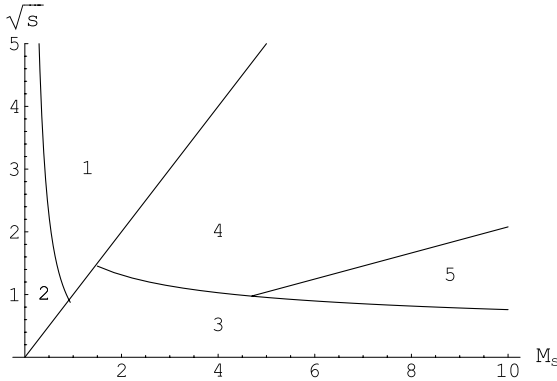


**Fig. 3.** The  $(\sqrt{s}, M_s)$ -plane for  $n = 3$  and  $M_D = 1$ . The *straight line* separating region 1 and 4 is  $\sqrt{s} = M_s$ , while the *straight line* separating region 4 and 5 is the line where the real and imaginary parts in (39) have equal magnitude. The *power-like curve* separating region 1 and 2 is  $\sqrt{s_{cd}}$  from (37) as a function of  $M_s$ , and the *line* separating the regions 4 and 5 from region 3 is the line where  $|A_{\text{Born}} X| = 1$ ; see (39). In the regions 1 and 2  $\sqrt{s}$  is larger than  $M_s$ , and, at least for  $\sqrt{s} \gg M_s$ , the eikonal approximation is correct. In region 1 the eikonal is, depending on  $b$ , either large compared to 1 or given by (32). In region 2 on the other hand the  $b$ -range where  $\chi$  is small includes a region where it is described by (33). In region 3 the corrections corresponding to higher order loops are small, but in region 4 they must be significant to assure unitarity

for when the eikonal approximation is relevant. As demonstrated in [9–11] the one-loop integral in (12) is dominated by the imaginary part given by (13). The contributions from multi-loop ladder diagrams (Fig. 1b) exponentiate, and the scattering amplitude is given by (14):

$$A_{\text{eik}}(k^2) = 2is \int d^2 \bar{b}_\perp e^{i\vec{k}_\perp \cdot \bar{b}_\perp} (1 - e^{i\chi}). \quad (36)$$

From (36) we see that the higher order corrections are important when  $\chi$  is of order 1 or larger. Correspondingly the Born term dominates when  $|\chi| < 1$ . We see from (33) and (34) that  $\chi$  varies only logarithmically when  $b$  is decreased below the point  $b = b_d$ . The importance of the higher order corrections for the integrated cross section therefore depends on whether or not  $|\chi(b_d)| > 1$ . This relation is satisfied whenever  $b_c > b_d$ , or equivalently when  $s > s_{cd}$ , with  $s_{cd}$  given by

$$s_{cd} = \frac{2}{(4\pi)^{\frac{n}{2}-1} \Gamma(\frac{n}{2})} \frac{M_D^{n+2}}{M_s^n}. \quad (37)$$

This defines the boundary between region 1 and region 2 in Fig. 3. In region 1 higher order terms are important for  $b < b_c$ , and the exponentiation in (36) is essential to keep the amplitude within the unitarity constraints.

The difference between regions 1 and 2 is illustrated in Fig. 4. Figure 4a corresponds to region 1, where the energy is high, and  $b_c > b_d$ . The absolute value of the eikonal  $\chi$  is smaller than 1 for  $b > b_c$ , and in this range the approximation in (32) is relevant. For  $b < b_c$ ,  $|\chi|$  is large and rapidly varying, which causes the exponent in (36) to oscillate rapidly.

Figure 4b corresponds to region 2. Here  $|\chi| < 1$  except in a very small region

$$b < \frac{1}{M_s} \exp\left(-\frac{4M_D^{n+2} \pi^{1-\frac{n}{2}}}{s M_s^n}\right) \quad (38)$$

around the origin. Therefore the Born term dominates the cross section, and higher order terms give only small corrections.

### 5.2 Non-eikonal regions, $s < M_s^2$

The Born amplitude in (24) is almost independent of the momentum exchange  $\vec{k}$  when  $k \ll M_s$ . When  $\sqrt{s} \ll M_s$  (regions 3, 4, and 5 in Fig. 3) this includes all kinematically allowed  $\vec{k}$ -values, which implies that the scattering is almost isotropic. Thus the exchange of the KK modes corresponds effectively to a contact interaction. (For wide-angle scattering we also expect corrections from spin polarization. This effect is neglected in the following.) The one-loop contribution in Fig. 1a is then represented by the diagram in Fig. 5a. We denote the momenta in the intermediate state  $P/2 \pm q$ , with  $P = p_1 + p_2$ , as indicated in Fig. 5a, and in the CMS we have  $P = (W, \vec{0})$ . The vertices are then given by the Born term in (24). The real part of the one-loop integral is logarithmically divergent, and in an effective field theory a cut-off is needed to get the observed gravitational interaction at

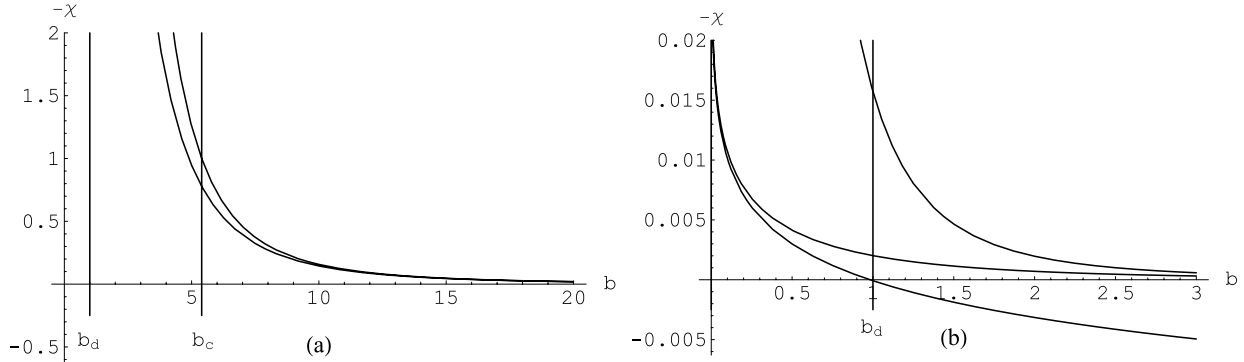


**Fig. 4.**  $-\chi$  as a function of impact parameter for two examples with  $n = 3$ . **a** High energies corresponding to region 1 in Fig. 3, with  $\sqrt{s} = 10$  TeV,  $M_s = 1$  TeV and  $M_D = 1$  TeV. The *upper curve* is the approximate expression in (30), and the *lower curve* the exact expression (39). **b** Kinematics corresponding to region 2 in Fig. 3,  $\sqrt{s} = 0.1$  TeV,  $M_s = 1$  TeV and  $M_D = 1$  TeV. The *upper curve* is the approximate high  $b$  expression in (32), the *lower curve* the approximate low  $b$  expression in (33) and the *interpolating line* is the exact expression in (29)

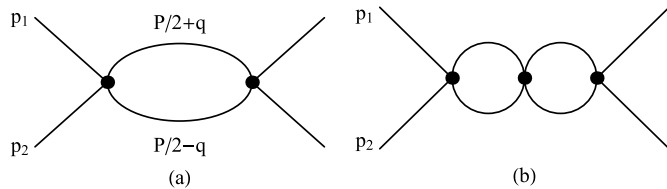


**Fig. 5.** When the exchanged momentum is small compared to  $M_s$ , the KK propagators are effectively replaced by vertex factors. The diagrams in Fig. 1 can then be drawn as above with only standard model particle lines

long (measurable) distances. We here expect this cut-off to be of order  $M_s$ , and the result is therefore given by

$$\begin{aligned}
 A_{1\text{-loop}}(k^2) &= \frac{-i}{2} \int_{q < M_s} \frac{d^4 q}{(2\pi)^4} A_{\text{Born}}^2 \frac{1}{(P/2 - q)^2} \frac{1}{(P/2 + q)^2} \\
 &\equiv A_{\text{Born}}^2 \cdot X, \\
 X &\approx \frac{1}{32\pi^2} \left( \ln \frac{4M_s^2}{s} + i\pi \right). \quad (39)
 \end{aligned}$$

We note here in particular that the result is a constant, independent of the momentum transfer  $k$ . Therefore also the one-loop amplitude can be effectively regarded as a contact term with a cut-off when  $k > M_s$ . The two-loop diagram in Fig. 5b can then be calculated in the same way as the one-loop diagram, and the result is

$$A_{2\text{-loop}} = A_{1\text{-loop}} \cdot A_{\text{Born}} X = A_{\text{Born}} \cdot (A_{\text{Born}} X)^2. \quad (40)$$

In the same way we can calculate ladder diagrams with more loops. Summing all ladders of this type we obtain

$$\begin{aligned}
 A_{\text{ladder}} &= A_{\text{Born}} (1 + A_{\text{Born}} X + (A_{\text{Born}} X)^2 + \dots) \\
 &= \frac{A_{\text{Born}}}{1 - A_{\text{Born}} X}. \quad (41)
 \end{aligned}$$

We see that instead of the exponent in the eikonal regime (where forward scattering dominates) we here obtain a geometric series from these ladder contributions. The

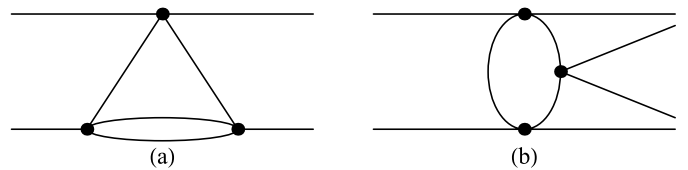


**Fig. 6.** **a** An example of a non-ladder diagram contributing to the elastic cross section in region 5 in Fig. 3. **b** An example of a diagram contributing to the inelastic cross section in region 5 in Fig. 3

importance of higher order corrections is in this approximation determined by the quantity  $A_{\text{Born}} X$ . When  $|A_{\text{Born}} X| \ll 1$  the Born term dominates. This corresponds to region 3 in Fig. 3.

When instead  $|A_{\text{Born}} X| > 1$ , we expect different results depending on whether it is the real or the imaginary part which dominates. When  $\ln(4M_s^2/s) < \pi$ , the imaginary part dominates the loop integral in (39). Thus this diagram is dominated by real intermediate states  $i$  in Fig. 1a, and we might expect that the ladder diagrams in Fig. 1b or Fig. 5b give the most important higher order corrections. This corresponds to region 4 in Fig. 3.

When  $\ln(4M_s^2/s) > \pi$  (region 5 in Fig. 3) the real part dominates the loop integral in (39). This indicates that inelastic scattering and virtual intermediate states are essential. Naturally a full understanding of these processes needs a theory for quantum gravity, but assuming that they can be described by an effective field theory, we will expect important contributions from more complicated, non-ladder, diagrams, like the examples shown in Fig. 6. For this reason we do not expect the result in (41) to be representative for a sum of all higher order corrections in this kinematical region.

## 6 Cross sections

Below we successively discuss the cross sections obtained in the five different regions in Fig. 3.



### 6.1 Region 1, $s > M_s^2$ and $|\chi(b_d)| > 1$

In this region  $s > M_s^2$  and  $\chi(b_d) > 1$ . As discussed in Sect. 5.1 the scattering is suppressed for  $-t > M_s^2$ . The first constraint therefore means that the cross section is dominated by small angle scattering, the imaginary part dominates the one-loop contribution, and the eikonal  $\chi(b)$  exponentiates. The cross section is then given by

$$\sigma = \int d^2\bar{b}_\perp 2 \operatorname{Re} \left( 1 - e^{i\chi(\bar{b}_\perp)} \right). \quad (42)$$

The effect of the constraint  $|\chi(b_d)| > 1$  was illustrated in Fig. 4a. It implies that  $b_d < b_c$ , and that the approximation  $\chi \approx -(b_c/b)^n$  in (32) is relevant for all  $b > b_c$ . In particular this means that, for  $b > b_c (> b_d)$ , we have  $|\chi| < 1$  and  $2 \operatorname{Re}(1 - e^{i\chi(\bar{b}_\perp)}) \approx \chi^2$ . For collisions with  $b < b_c$ , higher order loop corrections are important to satisfy unitarity. Here  $|\chi|$  is larger than 1 and rapidly varying, the exponent in (42) is oscillating, and therefore

$$\left\langle 2 \operatorname{Re} \left( 1 - e^{i\chi(\bar{b}_\perp)} \right) \right\rangle \approx 2. \quad (43)$$

Inserting these results into (42), we get (for  $n \geq 2$ ) the following result for the total cross section:

$$\begin{aligned} \sigma &\approx \int_0^{b_c} d^2b \cdot 2 + \int_{b_c}^\infty d^2b \left( \frac{b_c}{b} \right)^{2n} \\ &= \pi b_c^2 \left( 2 + \frac{1}{n-1} \right) = 2\pi b_c^2 \frac{n-1/2}{n-1}. \end{aligned} \quad (44)$$

When  $s$  is increased,  $\sigma$  grows proportional to  $b_c^2 \propto s^{2/n}$ . We note that the cross section is dominated by central collisions with  $b < b_c$  (especially for large  $n$ ), with only a small contribution from larger impact parameters. Integrating the constant 1 in the parentheses in (36) between 0 and  $b_c$  gives a dominant forward peak, with oscillations at larger angles. The amplitude for these oscillations falls off proportional to  $1/k^{3/2}$ , corresponding to  $d\sigma/dt \propto 1/k^3$  for the cross section.

For large  $k$  the dominant contribution in (36) comes from the term  $e^{i\chi}$  and a small range of  $b$ -values around  $b_s$ , where

$$b_s = b_c \left( \frac{n}{k b_c} \right)^{\frac{1}{n+1}}. \quad (45)$$

For these  $b$ -values the frequencies of the exponents  $e^{i\bar{k}\cdot\bar{b}}$  and  $e^{i\chi(\bar{b})}$  in (36) oscillate in phase, which gives an enhanced contribution. Using the saddle-point approximation we get from this contribution (apart from logarithmic corrections) a cross section which falls off like  $d\sigma/dt \propto 1/t^{\frac{n+2}{n+1}}$ . This contribution is dominating for  $k > n/b_c$ , where  $|\chi(b_s)| > 1$ . As pointed out in [4] it corresponds to classical scattering in a  $1/r^{n+1}$  potential. For small scattering angles  $\theta$  we have for a non-relativistic particle with

mass  $m_1$  moving with constant speed  $v$  and momentum  $p = m_1 v$  in the potential of a mass  $m_2$

$$\begin{aligned} \theta &\approx \frac{|\bar{p}_\perp|}{|\bar{p}|} = \frac{1}{|\bar{p}|} \int_{-\infty}^\infty dt F_\perp(r) \\ &= -G_{N(4)} R^n S_n \Gamma(n) \frac{m_1 m_2}{m_1 v} \int_{-\infty}^\infty \frac{dr}{v} \frac{d}{db} \left( \frac{1}{\sqrt{r^2 + b^2}} \right)^{n+1} \\ &= \frac{n(2\sqrt{\pi})^n \Gamma(\frac{n}{2})}{8\pi v^2} \frac{m_2}{M_D^{n+2}} \frac{1}{b^{n+1}}. \end{aligned} \quad (46)$$

From this we see that if  $m_1 = s/(4m_2)$

$$b_{\text{nonrel}} = b_c \left( \frac{n}{4vp b_c} \right)^{\frac{1}{n+1}}, \quad (47)$$

agreeing parametrically with (45). (A numerical difference is expected since (45) is ultra-relativistic whereas (47) is a non-relativistic result.) This behavior is discussed in more detail in [4], and we note that in this region, where  $s$  is much larger than both  $M_s^2$  and  $s_{\text{cd}}$ , our result is consistent with the result of this reference. A necessary condition is, however, that  $\sqrt{s}$ ,  $M_D$ , and  $M_s$  have values such that  $b_s > b_d = 1/M_s$ , which for fixed  $k$ -value gives a minimum value for  $M_s$ . If this relation is not satisfied, the phase variation in  $\exp(i\chi)$  is given by (33) rather than (32), and therefore we do not get the phase coherence in the integral in (36).

### 6.2 Region 2, $s > M_s^2$ and $|\chi(b_d)| < 1$

In region 2,  $s$  is larger than  $M_s^2$  but smaller than  $s_{\text{cd}}$ , and therefore  $b_d > b_c$ . A typical example is illustrated in Fig. 4b. We see here that  $|\chi|$  is small compared to 1, apart from the logarithmic peak for very small  $b$ . The influence of the small  $b$  peak is also suppressed by a phase space factor proportional to  $b db$ . The cross section is therefore well approximated by the Born amplitude.

The largest contributions to the cross section come from  $b$ -values in the neighborhood of  $b_d$ ; for larger  $b$ ,  $\chi$  falls off  $\propto (b_c/b)^n$ , and for smaller  $b$  the scattering is limited by the smaller phase space  $\sim b db$ . These  $b$ -values are just in the transition region between the two asymptotic forms in (32) and (33). To get a good estimate of the cross section we should therefore use the exact expression for  $\chi$  in (29). For an order of magnitude estimate we may, however, approximate  $\chi$  by the asymptotic result  $\chi \approx -(b_c/b)^n$  for  $b > b_d$ , and by a constant  $= -(b_c/b_d)^n$  for all  $b < b_d$ . This gives the following qualitative estimate for the total cross section:

$$\begin{aligned} \sigma &\sim \int_0^{b_d} d^2b \left( \frac{b_c}{b_d} \right)^{2n} + \int_{b_d}^\infty d^2b \left( \frac{b_c}{b} \right)^{2n} \\ &= \pi \frac{b_c^{2n}}{b_d^{2n-2}} \frac{n}{n-1}. \end{aligned} \quad (48)$$

As  $b_c \sim (s/M_D^{n+2})^{1/n}$ , and  $b_d = 1/M_s$ , we note that the cross section grows  $\propto s^2 M_s^{2n-2}/M_D^{2n+4}$ . Thus, although

the cross section is comparatively small in this region, it has a stronger growth rate  $\propto s^2$  than in region 1.

For the differential cross section, we note that the  $t$ -channel Born amplitude is proportional to  $1/k^2$  for  $-k^2 \gg M_s^2$ . This implies that the cross section has a forward peak. It corresponds to scattering at distances small compared to  $1/M_s$ , in the  $1/r$  potential from (27). There is however no forward divergence since the growth is softened at  $-k^2 \sim M_s^2$ , i.e. at distances comparable to the brane thickness.

### 6.3 Region 3, $s < M_s^2$ and $|A_{\text{Born}}X| < 1$

In region 3 the cross section is also dominated by the Born amplitude. But in this case the scattering is almost isotropic (apart from spin dependences) as the factor  $-k^2$  in the propagator is small compared to the heavier and most important KK modes. This implies that we may also have important contributions from  $u$ - and  $s$ -channel exchanges. For identical particles, the  $u$ -channel contribution has the same magnitude as that from  $t$ -channel.

### 6.4 Region 4, $s < M_s^2$ , $|A_{\text{Born}}X| > 1$ and $\text{Im}(X) > \text{Re}(X)$

The one-loop  $t$ -type contribution in Fig. 5a is dominated by the imaginary part, originating from real intermediate states. If loop diagrams of this type dominate (and we can neglect the angular dependence due to spin effects) the all-loop amplitude can be approximated by the geometric sum in (39). As in region 3, the result is then approximately isotropic, but here the Born contribution is suppressed by the higher order corrections. For identical particles the  $u$ -type ladder is identical to the  $t$ -type ladder and hence equally important. For identical particle–antiparticle pairs also  $s$ -channel contributions have to be considered.

### 6.5 Region 5, $s < M_s^2$ , $|A_{\text{Born}}X| > 1$ and $\text{Im}(X) < \text{Re}(X)$

This region corresponds to situations where the effective cut-off  $M_s$  is large (“narrow brane” or strong “brane tension”) and the energy is in an intermediate range. From Fig. 3 we see that for e.g.  $n = 3$   $M_s$  must be larger than  $5M_D$ . The one-loop diagram has a dominant real part, which implies that virtual intermediate states and inelastic reactions are important. Therefore non-ladder diagrams are expected to give large contributions, and we showed two examples in Fig. 6. This region may consequently be much more complicated than the other kinematical regions, and more sensitive to unknown features of quantum gravity. In this paper we will therefore not make any specific predictions for what might be expected in this kinematic region.

## 7 Conclusions

In the ADD model it is assumed that standard model particles live on a 4-dimensional brane, embedded in a  $(4+n)$ -dimensional space with  $n$  compactified dimensions. In these, only the gravitational field is allowed to propagate. If the brane is infinitely thin and infinitely rigid, the exchange of very massive Kaluza–Klein modes represents a contact interaction of infinite strength between the standard model particles. This is not physically acceptable and different ideas have been proposed to regularize the scattering process.

If the brane has a finite width, or if it is not infinitely well localized, the exchange of KK modes will be suppressed for KK wavelengths shorter than the width of the brane, or the size of its fluctuations. If gravitational interaction can be described by an effective field theory, we then expect an effective cut-off (denoted  $M_s$ ) for high KK masses, which does not have to be of the same magnitude as the fundamental Planck mass  $M_D$ .

In this paper we have studied the effect of such a cut-off on the scattering of standard model particles at various energies. We find that several troublesome infinities and divergences are removed. The scattering process depends on three different energy scales, the collision energy  $\sqrt{s}$ , the fundamental Planck scale  $M_D$ , and the cut-off scale  $M_s$ . The Planck scale,  $M_D = (8\pi R^n G_{N(4)})^{-1/(n+2)}$ , depends on the compactification radius  $R$  of the extra dimensions and the magnitude of Newton’s constant, while the effective cut-off depends on the width of the brane,  $M_s \sim (\text{brane thickness})^{-1}$ , or the fluctuations in its position. These scales are thus not automatically related. Clearly the compactification scale  $R$  must be larger than the brane width  $1/M_s$ .

Depending on the relative magnitude between these scales, we have here studied five different kinematical regions with different dynamical behavior. In one region (region 1 in Fig. 3), the scattering is dominated by small angles, and the eikonal approximation is applicable. Here we recognize classical scattering in a  $1/r^{n+1}$  potential and the results of Giudice–Rattazzi–Wells [4]. In two other regions (2 and 3 in Fig. 3) the Born approximation is applicable. In one of these (region 2) forward scattering dominates and corresponds to scattering in a  $1/r$  potential, but with a coupling enhanced by a factor proportional to  $\left(\frac{\text{compactification radius}}{\text{brane width}}\right)^n$  compared to scattering in the ordinary  $1/r$  Newtonian large distance potential. In the other Born region (region 3) the scattering is approximately isotropic, as expected in [5, 6]. In a fourth region it is suggested that the exponentiation from ladder-type diagrams in the eikonal region is replaced by a geometric sum. The scattering is expected to be mostly elastic, since on-shell intermediate states dominate, but approximately isotropic. In the last region inelastic processes and non-ladder loop diagrams are important and make predictions very difficult. The boundaries between the different regions are expressed in the three mass scales involved, as illustrated in Fig. 3.

*Acknowledgements.* We thank Leif Lönnblad and Johan Bijnens for useful discussions.

## References

1. N. Arkani-Hamed, S. Dimopoulos, G.R. Dvali, Phys. Lett. B **429**, 263 (1998) [hep-ph/9803315]
2. N. Arkani-Hamed, S. Dimopoulos, G.R. Dvali, Phys. Rev. D **59**, 086004 (1999) [hep-ph/9807344]
3. I. Antoniadis, N. Arkani-Hamed, S. Dimopoulos, G.R. Dvali, Phys. Lett. B **436**, 257 (1998) [hep-ph/9804398]
4. G.F. Giudice, R. Rattazzi, J.D. Wells, Nucl. Phys. B **630**, 293 (2002) [hep-ph/0112161]
5. T. Han, J.D. Lykken, R.-J. Zhang, Phys. Rev. D **59**, 105006 (1999) [hep-ph/9811350]
6. G.F. Giudice, R. Rattazzi, J.D. Wells, Nucl. Phys. B **544**, 3 (1999) [hep-ph/9811291]
7. G.F. Giudice, A. Strumia, Nucl. Phys. B **663**, 377 (2003) [hep-ph/0301232]
8. D. Atwood, S. Bar-Shalom, A. Soni, Phys. Rev. D **62**, 056008 (2000) [hep-ph/9911231]
9. R.I. Glauber, Lectures in Theoretical Physics (Interscience Publisher, NY, 1959)
10. R. Blankenbecler, M.L. Goldberger, Phys. Rev. **126**, 766 (1962)
11. R.C. Arnold, Phys. Rev. **153**, 1523 (1967)
12. R. Emparan, G.T. Horowitz, R.C. Myers, Phys. Rev. Lett. **85**, 499 (2000) [hep-th/0003118]
13. S. Dimopoulos, G. Landsberg, Phys. Rev. Lett. **87**, 161602 (2001) [hep-ph/0106295]
14. S.B. Giddings, S. Thomas, Phys. Rev. D **65**, 056010 (2002) [hep-ph/0106219]
15. P. Kanti, Int. J. Mod. Phys. A **19**, 4899 (2004) [hep-ph/0402168]
16. L. Lönnblad, M. Sjö Dahl, T. Akesson, JHEP **09**, 019 (2005) [hep-ph/0505181]
17. C.M. Harris, P. Kanti, JHEP **10**, 014 (2003) [hep-ph/0309054]
18. M. Bando, T. Kugo, T. Noguchi, K. Yoshioka, Phys. Rev. Lett. **83**, 3601 (1999) [hep-ph/9906549]
19. T. Kugo, K. Yoshioka, Nucl. Phys. B **594**, 301 (2001) [hep-ph/9912496]
20. M. Sjö Dahl, Eur. Phys. J. C **50**, 679 (2007)